

Transport and Damping from Rotational Pumping in Magnetized Electron Plasmas

B. P. Cluggish and C. F. Driscoll

Department of Physics, 0319, University of California at San Diego, La Jolla, California 92093

(Received 7 December 1994)

Radial particle transport and the damping of the $m = 1$ diocotron mode from “rotational pumping” have been measured on a magnetized electron column. Rotational pumping is collisional dissipation of the axial compressions caused by $\mathbf{E} \times \mathbf{B}$ rotation of the column through asymmetric confining potentials. The observed transport rates are in close agreement with theory.

PACS numbers: 52.25.Wz, 51.20.+d, 52.20.Fs, 52.25.Fi

Collisional cross-field transport due to electric or magnetic field asymmetries is important in many neutral and non-neutral plasma confinement devices. In magnetic mirrors, it has long been postulated that particles resonant with field asymmetries enhance radial diffusion [1], but experimental verification [2] is difficult. In tokamaks, “magnetic pumping” by a spatially varying magnetic field is thought to dissipate poloidal rotation [3]. In non-neutral traps, confinement times much greater than the rotation and transit times are important for a number of technologies and experiments [4–6]; but trap asymmetries can degrade confinement [7,8]. Non-neutral plasmas are often approximated as 2D guiding center fluids [9,10] on the rotational time scale, with 3D collisions causing dissipative or viscous effects [11,12].

Here, we present measurements of radial particle transport and resulting mode damping from “rotational pumping” of a magnetized electron column displaced from the axis of a cylindrical trap. Rotational pumping is the collisional dissipation of the axial compressions which are caused by $\mathbf{E} \times \mathbf{B}$ rotation of the column through asymmetric confinement potentials; here, the confinement potentials appear asymmetric only because of the displacement of the column away from the symmetry axis of the trap. We find that this transport conserves particle number, conserves angular momentum by moving

the column back to the trap axis as the column expands, and conserves total energy by dissipating electrostatic energy into thermal energy. This dissipation is analogous to that caused by the “second” or “bulk” viscosity [13] in polyatomic gases, which causes weak absorption of sound waves [14]; here, it causes readily measured particle transport. The transport rate is proportional to the electron-electron collision rate, which drops precipitously in the cryogenic, strongly magnetized regime; surprisingly, the transport is otherwise independent of the magnetic field strength. The observed transport rates are in close agreement with a new theory by Crooks and O’Neil [15].

We confine the electron plasmas in a Penning-Malmberg trap [16,17], shown schematically in Fig. 1. Electrons from a tungsten filament are confined in a series of conducting cylinders of radius $R_w = 1.27$ cm, enclosed in a vacuum can at 4.2 K. The electrons are confined axially by negative voltages $V_c = -200$ V on cylinders 1 and 4; radial confinement is provided by a uniform axial magnetic field, with $10 < B < 60$ kG. The trapped plasma typically has initial density $10^9 \leq n \leq 10^{10}$ cm $^{-3}$, rms radius $R_p \sim 0.04$ cm, and length $L_p \sim 3$ cm, with a characteristic expansion time $10^2 \leq \tau_m < 10^3$ sec. The apparatus is operated in an inject-manipulate-dump cycle and has a shot-to-shot reproducibility of $\delta n/n \sim 1\%$.

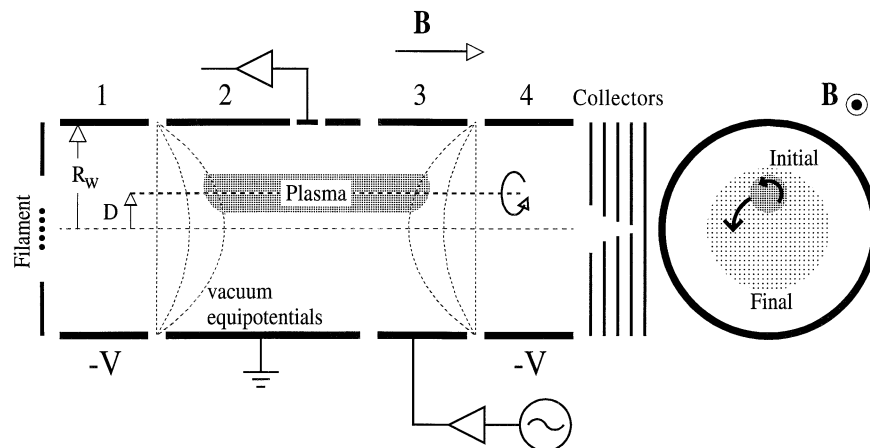


FIG. 1. Schematic of the cylindrical apparatus and electron plasma. End view shows initial and final plasma states.

The self-electric-field of the electrons causes an $\mathbf{E} \times \mathbf{B}$ drift rotation around an axis through the center of charge, at a rate $500 \leq f_E \leq 3000$ kHz. When the column is displaced from the center of the trap, image charges in the conducting walls cause the column to orbit around the trap axis in the $m = 1$ “diocotron” mode, at frequency $5 \leq f_d \leq 20$ kHz. The image charge signal received on a wall sector is proportional to the displacement D of the column from the trap axis.

The density of the plasma is measured by dumping the electrons onto the end collectors, by grounding cylinder 4. A rough histogram is obtained from the charge on the 5 collectors. We obtain a more accurate z -integrated density $q(\rho)$ using many shots and varying the displacement of the column. Here, ρ refers to the radius from the plasma axis, i.e., $\mathbf{r} = \mathbf{D} + \boldsymbol{\rho}$. The parallel plasma temperature T_{\parallel} is measured by slowly ramping the voltage on cylinder 4 to ground, and measuring the number of electrons which escape as a function of the confining voltage. We can have $0.003 \leq T_{\parallel} \leq 20$ eV, giving axial electron bounce frequencies $4 \times 10^5 \leq f_b \leq 3 \times 10^7$ Hz, and T_{\parallel} to T_{\perp} collisional equilibration rates $10^3 \leq \nu_{\perp\parallel} \leq 10^5 \text{ sec}^{-1}$.

We calculate the 3D plasma density $n(x, y, z)$ and potential $\phi(x, y, z)$ from the measured $q(\rho)$, D , and T_{\parallel} by numerically solving Poisson’s equation on a $125 \times 125 \times 200$ grid. Here, we assume

$$n(x, y, z) = n_0(x, y) \exp\{e\phi(x, y, z)/kT_{\parallel}\}, \quad (1)$$

where $n_0(x, y)$ follows from $\int dz n(x, y, z) = q(\rho)$, with $\rho^2 = (x - D)^2 + y^2$.

Figure 2 shows a typical evolution of the density profile $n(\rho, z = 0)$ of an off-axis column. The rms radius R_p increases from 0.044 cm at $t = 0$ to 0.22 cm at $t = 10$ sec, while the central density decreases a factor of 8. However, the total number of particles N is conserved to within 1%.

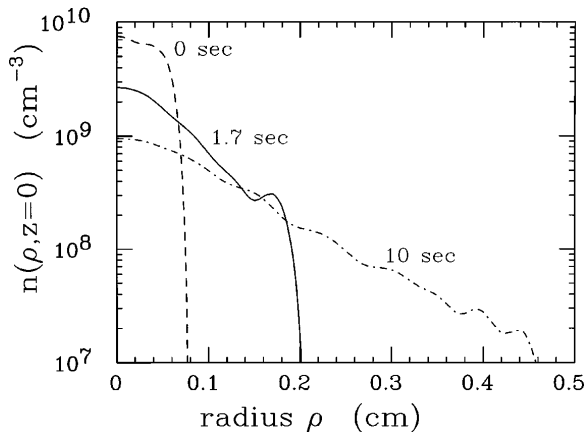


FIG. 2. Measured plasma density profiles at three different times as rotational pumping causes plasma expansion.

The displacement D decreases as the plasma expands, damping the $m = 1$ diocotron mode. In these strongly magnetized plasmas, the total angular momentum is dominated by the electromagnetic component, i.e.,

$$P_{\theta} \equiv \int d^3\mathbf{r} n \left(m v_{\theta} r - \frac{eB}{2c} r^2 \right) \approx \frac{eB}{2c} N [D^2 + R_p^2],$$

where $R_p^2 \equiv (1/N) \int 2\pi\rho d\rho \rho^2 q(\rho)$ is the mean square radius of the plasma. Figure 3(a) shows $(D/R_w)^2$, $(R_p/R_w)^2$, and their sum for the evolution of Fig. 2. Initially, 97% of P_{θ} is in $(D/R_w)^2$; after 10 sec, expansion and mode damping leave only 1% of P_{θ} in $(D/R_w)^2$. The sum of the two P_{θ} components remains constant, implying that the forces causing the transport are azimuthally symmetric around the trap axis.

This expansion and symmetrization process converts electrostatic energy H_{ϕ} into kinetic energy H_k . We also calculate the total radiated energy H_{rad} and the work done on the power supplies which provide the confining potentials, W_{ps} , as

$$H_{\phi} = -\frac{1}{2} \int d^3x n(x, y, z) e\pi(x, y, z)/N,$$

$$H_k = \frac{1}{2} k(T_{\parallel} + 2T_{\perp}), \quad H_{\text{rad}} = \frac{3}{2} \int_0^t dt' kT_{\perp}/\tau_{\text{rad}},$$

$$W_{\text{ps}} = -\frac{1}{2} \Delta Q V_c/N.$$

Here, $\Delta Q(t)$ is the change in the charge on the end cylinders, and τ_{rad} is the energy loss time of the electrons due to cyclotron radiation. At $B = 40$ kG, we measure $\tau_{\text{rad}} = 0.29$ sec [16], about 25% longer than predicted by the Larmor formula for an electron in free space. Because

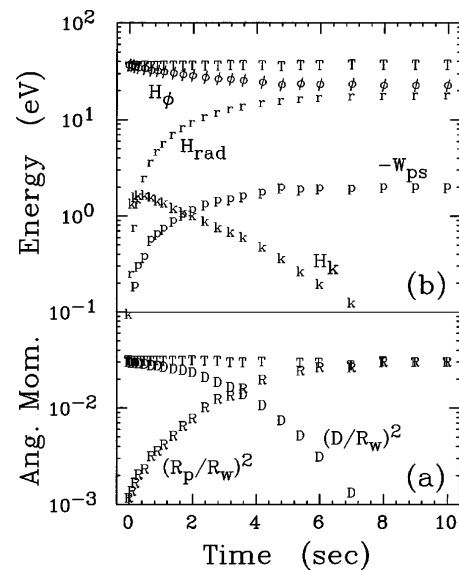


FIG. 3. Constancy of total angular momentum and energy, from (a) plasma diameter and displacement components of P_{θ} , and (b) electrostatic, radiated, kinetic, and power supply components of total energy.

$\tau_{\text{rad}} \gg \nu_{\perp\parallel}^{-1}$, we assume that $T_{\perp} \approx T_{\parallel} \equiv T$ in calculating H_k and H_{rad} .

Figure 3(b) shows the evolution of H_{ϕ} , H_t , W_{ps} , H_{rad} , and their sum. Over 10 sec, H_{ϕ} decreases by 40% from its initial value. H_k increases from 0.09 to 1.6 eV during the first 0.5 sec, after which radiative cooling dominates. The dissipation of electrostatic into kinetic energy indicates that $\mathbf{E} \times \mathbf{B}$ drift dynamics alone cannot be responsible for the observed transport. The constancy of the total energy indicates that the plasma is not coupled to any unknown energy sources or sinks.

We characterize this transport by the damping rate of the $m = 1$ diocotron mode, γ , i.e., by the rate of decrease of the column displacement D . For $D_0 \leq R_p$, the displacement decreases as $D(t) = D_0 \exp(-\gamma t)$.

We find that the transport exhibits several striking parameter dependences. One is that γ is nearly independent of magnetic field for moderate temperatures. As B is varied from 10 to 60 kG, we find that γ decreases only 30%. This is in contrast with "conventional" transport scaling as B^{-2} [8,18] or B^{-1} [11], generally due to dependence on the cyclotron radius r_c , or on $\mathbf{E} \times \mathbf{B}$ drift velocities.

Even more striking is the dependence of γ on plasma temperature for small T , as shown in Fig. 4. As T is decreased from 0.01 to 0.003 eV, we find that γ decreases by 2 orders of magnitude. In this highly magnetized regime, $\nu_{\perp\parallel}$ becomes exponentially small [17] because the cyclotron radius is smaller than the distance of closest approach, i.e., $r_c < b \equiv e^2/kT$. This precipitous drop in γ is a strong indication that $\gamma \propto \nu_{\perp\parallel}$. The decrease in γ for $T > 0.1$ eV is also consistent with this dependence, since $\nu_{\perp\parallel} \propto T^{-3/2}$ for high T . Experimentally, we maintain a constant plasma temperature by applying a 2 MHz oscillation to cylinder 3, thus balancing the radiative cooling. We observe that γ is independent of the frequency and amplitude of the heating oscillation, except through the plasma temperature.

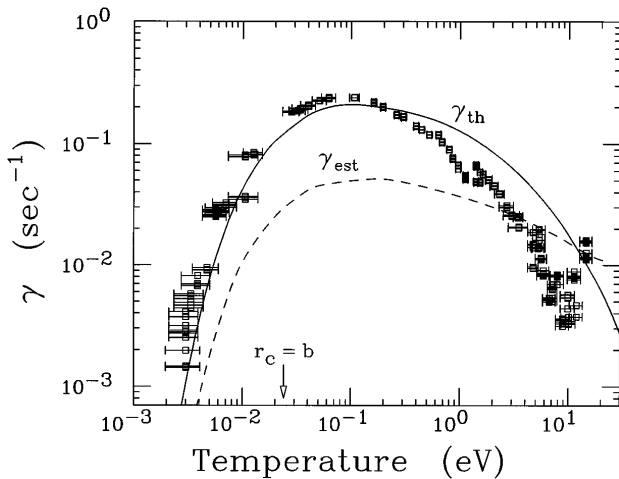


FIG. 4. Measured transport and damping rate γ versus plasma temperature, with estimated and calculated theory predictions.

The recent theory of rotational pumping by Crooks and O'Neil analyzes the cyclic variation in the length of a tube of plasma as it $\mathbf{E} \times \mathbf{B}$ drifts around the plasma axis. They assume that the Debye length is small, i.e., $\lambda_D \ll L_p$. In this approximation, ϕ is uniform in z inside the plasma and abruptly increases at the ends, so the bounce length of an electron is independent of its energy. The length at radius ρ thus varies as

$$L(\rho, t) = L_0(\rho) + \delta L(\rho) \sin \omega_R t, \quad (2)$$

where $\delta L \ll L_0$ and $\omega_R(\rho)/2\pi \equiv f_E(\rho) - f_d$ is the rotation frequency of the plasma in the diocotron mode frame. The modulation in L causes a modulation in T_{\parallel} , but collisions tend to equilibrate T_{\perp} and T_{\parallel} , causing an irreversible increase in both. Ignoring radiation, T_{\parallel} varies as

$$\frac{dT_{\parallel}(\rho, t)}{dt} = 2\nu_{\perp\parallel}(T_{\perp} - T_{\parallel}) - \frac{2}{L} \frac{dL}{dt} T_{\parallel}. \quad (3)$$

Expanding T_{\parallel} (and T_{\perp}) in orders of $\delta L/L_0$ as $T_{\parallel} = T_{\parallel}^{(0)} + T_{\parallel}^{(1)} + \dots$ gives $T_{\parallel}^{(0)} = T_{\perp}^{(0)} = T(\rho)$. In first order, $T_{\parallel}^{(1)}$ is partially out of phase with $L(\rho, t)$. This phase difference gives an irreversible heating in second order in Eq. (3). The rate of expansion of the plasma column is then obtained by averaging the rate of change of thermal energy over a plasma rotation, and equating it to the rotation-averaged Joule heating caused by radial transport. Assuming $\omega_R \gg \nu_{\perp\parallel}$, this gives

$$-e\langle \Gamma_{\rho} E_{\rho} \rangle = \frac{3}{2} n \left\langle \frac{d}{dt} T_{\parallel}^{(2)} \right\rangle = 2nT\nu_{\perp\parallel} \left(\frac{\delta L}{L_0} \right)^2. \quad (4)$$

Here, E_{ρ} is the radial electric field and Γ_{ρ} is the radial electron flux in the diocotron mode frame. Further, Crooks and O'Neil assume that $\omega_b \gg \omega_R$, giving n , T , Γ_{ρ} , and E_{ρ} uniform along the field lines; this is weakly satisfied in our experiments. The predicted damping rate γ can be calculated from Γ_{ρ} , using the continuity equation and conservation of P_{θ} , as

$$\gamma \equiv \frac{1}{D^2} \frac{dR_p^2}{dt} \equiv \frac{2\pi}{ND^2} \int \rho d\rho dz \rho^2 \frac{1}{\rho} \frac{\partial}{\partial \rho} \rho \Gamma_{\rho}. \quad (5)$$

Equation (5) can be integrated analytically if we assume uniform density and temperature, and approximate δL by $\delta L = \kappa(D/R_w)\rho$, where $\kappa \sim 2$ [19]. We then obtain an estimated damping rate

$$\gamma_{\text{est}} = 4\kappa^2 \nu_{\perp\parallel} \frac{\lambda_D^2 R_p^2}{L_p^2 R_w^2} \frac{1}{1 - 2R_p^2/R_w^2}. \quad (6)$$

γ_{est} is independent of D and depends on B only through the Coulomb logarithm in $\nu_{\perp\parallel}$ [17]. We have plotted γ_{est} in Fig. 4 as a dashed curve. It agrees with our data within a factor of 6.

A more accurate theoretical prediction γ_{th} is obtained using δL from the measured $q(\rho)$ and Eq. (1); then, numerical integration of Eq. (5) gives the solid curve in Fig. 4, which shows closer agreement with the data. The difference in slope between γ_{est} and γ_{th} for $T > 1$ eV is due to a decrease in the actual δL with temperature: higher energy electrons penetrate farther towards the end cylinders, where the vacuum equipotential surfaces have less curvature, as shown in Fig. 1. We postulate two reasons why γ_{th} is up to twice as large as the measured γ for $T > 0.2$ eV in Fig. 4. First, at high enough temperatures, $\lambda_D > \delta L$, so the electron bounce length may not be well described by Eq. (2). Second, the measured (central) temperature may underestimate the true average temperature.

In addition to D , B , and T , we have measured the dependence of γ on V_c , n , R_p , and L_p . In all cases, we find agreement between γ_{th} and experiment comparable to the agreement in Fig. 4. Crooks and O'Neil also predict that when $\omega_b < \omega_R$ the transport may be enhanced greatly by electrons whose bounce and rotation frequencies are resonant. We do not observe any enhancement, but these resonances should not exist in our experiments, since $\omega_b \approx \nu_{\perp\parallel}$ when $\omega_b < \omega_R$.

The unusual temperature dependence of γ can result in complex, nonlinear behavior when $r_c \leq b$ holds. If the Joule heating in Eq. (4) is larger than kT/τ_{rad} , then γ and T will unstably increase, saturating when $r_c \approx b$; otherwise, γ and T will unstably decrease until T approaches the 4.2 K wall temperature. This can cause a bifurcation in the time evolution of D . Thereafter, fluctuations in γ can cause transitions between the two saturated states because the difference in kT between states is small compared to the electrostatic energy. Furthermore, if a resistive wall destabilizes the diocotron mode, a complicated nonlinear "dance" with both positive and negative γ can result [20].

From a fluid perspective, rotational pumping can be thought of as dissipation of a compressible flow by a second viscosity ζ , where the dissipation rate is $\gamma \propto \zeta(\nabla\mathbf{v})^2$. In the guiding center approximation, the cyclotron motion of the electrons is a "hidden" degree of freedom, like the vibrations and rotations of gas molecules [14]. Equilibration of hidden and translational degrees of freedom gives rise to a second viscosity [13]. The second viscosity coefficient in these plasmas can be expressed as

$$\zeta = \frac{4}{9} \frac{nT}{\nu_{\perp\parallel}} \frac{1}{1 + (\omega_R/3\nu_{\perp\parallel})^2}. \quad (7)$$

In our experiments, γ is independent of ω_R because $\omega_R \gg \nu_{\perp\parallel}$ and $(\nabla \cdot \mathbf{v})^2 \propto \omega_R^2$.

This rotational pumping mechanism should also damp the $m \geq 2$ diocotron modes. It may also cause the dissipation of several otherwise stable non-neutral plasma configurations, including two electron vortex equilibria

[21], vortex crystals [22], asymmetric equilibria [10], and toroidal electron plasmas [23]. Rotational pumping is analogous to magnetic pumping which is presumed to strongly damp poloidal rotation in tokamaks [3]. Similarly, rotational pumping should strongly damp azimuthal rotation in nonaxisymmetric systems such as tandem mirrors [1,2].

The authors would like to acknowledge experimental suggestions by the late J. H. Malmberg, and enlightening discussions with T. B. Mitchell and K. S. Fine. This work was supported by NSF PHY91-20240 and ONR N00014-89-J-1714.

-
- [1] D. D. Ryutov and G. V. Stupakov, *Fiz. Plazmy* **4**, 521 (1978).
 - [2] D. L. Goodman, C. C. Patty, and R. S. Post, *Phys. Fluids B* **2**, 2173 (1990); E. B. Hooper *et al.*, *Phys. Fluids* **28**, 3609 (1985); H. D. Price *et al.*, *Nucl. Fusion* **23**, 1043 (1983).
 - [3] T. H. Stix, *Phys. Fluids* **16**, 1260 (1973); W. M. Stacey and D. R. Jackson, *Phys. Fluids B* **5**, 1828 (1993).
 - [4] G. Gabrielse *et al.*, *Phys. Rev. Lett.* **65**, 1317 (1990).
 - [5] D. J. Wineland *et al.*, *Phys. Rev. Lett.* **67**, 1735 (1991).
 - [6] R. W. Gould and M. A. LaPointe, *Phys. Rev. Lett.* **67**, 3685 (1991).
 - [7] D. L. Eggleston and J. H. Malmberg, *Phys. Rev. Lett.* **59**, 1675 (1987).
 - [8] C. F. Driscoll, K. S. Fine, and J. H. Malmberg, *Phys. Fluids* **29**, 2015 (1986).
 - [9] X.-P. Huang and C. F. Driscoll, *Phys. Rev. Lett.* **72**, 2187 (1994); T. B. Mitchell *et al.*, *ibid.* **73**, 2196 (1994).
 - [10] J. Notte, A. J. Peurrung, and J. Fajans, *Phys. Rev. Lett.* **69**, 3056 (1992); J. Notte and J. Fajans, *Phys. Plasmas* **1**, 1123 (1994).
 - [11] C. F. Driscoll, J. H. Malmberg, and K. S. Fine, *Phys. Rev. Lett.* **60**, 1290 (1988).
 - [12] T. M. O'Neil *et al.*, in *Turbulence and Anomalous Transport in Magnetized Plasmas*, edited by D. Gresillon (Editions de Physique, Orsay, 1987), pp. 293-308.
 - [13] L. D. Landau and E. M. Lifshitz, *Fluid Mechanics* (Pergamon, Oxford, England, 1987), 2nd ed., Sec. 81.
 - [14] J. D. Lambert, *Vibrational and Rotational Relaxation in Gases* (Clarendon, Oxford, England, 1977), Sec. 2.2.
 - [15] S. M. Crooks and T. M. O'Neil, *Phys. Plasmas* (to be published).
 - [16] B. R. Beck, Ph.D. dissertation, UCSD, 1990.
 - [17] B. R. Beck, J. Fajans, and J. H. Malmberg, *Phys. Rev. Lett.* **68**, 317 (1992).
 - [18] J. H. Malmberg and C. F. Driscoll, *Phys. Rev. Lett.* **44**, 654 (1980).
 - [19] A. J. Peurrung and J. Fajans, *Phys. Fluids B* **5**, 4250 (1993); A. J. Peurrung and J. Fajans, *ibid.* **5**, 4295 (1993).
 - [20] J. Helffrich, B. Cluggish, and J. H. Malmberg, *Bull. Am. Phys. Soc.* **36**, 2331 (1991).
 - [21] T. B. Mitchell, C. F. Driscoll, and K. S. Fine, *Phys. Rev. Lett.* **71**, 1371 (1993).
 - [22] K. S. Fine, C. F. Driscoll, and A. C. Cass, *Bull. Am. Phys. Soc.* **39**, 1736 (1994).
 - [23] S. S. Khirwadkar *et al.*, *Phys. Rev. Lett.* **71**, 3443 (1993).